Supplementary Information

Bioimaging of glutathione variation for early diagnosis of hepatocellular carcinoma using a liver-targeting ratiometric near-infrared fluorescent probe

Xiaoyue Han, [†a] Yanlong Xing,[*†b,c] Xinyu Song,[d] Kun Dou,[b,c] Fabiao Yu,[*b,c] Lingxin Chen[*a]

a. CAS Key Laboratory of Coastal Environmental Processes and Ecological Remediation, Yantai Institute of Coastal Zone Research, Chinese Academy of Sciences, Yantai 264003, China

b. Key Laboratory of Hainan Trauma and Disaster Rescue, The First Affiliated Hospital of Hainan Medical University, Hainan Medical University, Haikou 571199, China

c. Engineering Research Center for Hainan Bio-Smart Materials and Bio-Medical Devices, Key Laboratory of Hainan Functional Materials and Molecular Imaging, Key Laboratory of Emergency and Trauma, Ministry of Education, College of Emergency and Trauma, Hainan Medical University, Haikou 571199, China

d. State Key Laboratory of Respiratory Disease, Guangzhou Institute of Respiratory Health, National Clinical Research Center for Respiratory Disease, The First Affiliated Hospital of Guangzhou Medicine University, Guangzhou 510120, China

† F X. Han and Y. Xing contributed equally.

Contents:

1. General methods
2. The synthesis of the probe **CyO-Disu**.
3. Effect of pH values to **CyO-Disu** and CyO
4. Selectivity of **CyO-Disu** toward various reactive substances
5. Reaction kinetics of **CyO-Disu** towards GSH
6. MTT assay for **CyO-Disu**
7. Quantitative assay of GSH concentration of various cells in Fig. 2a
8. Sublocation in Cells
9. Bright-field images of Fig. 2 and Fig. 3
10. H&E-stained liver tissues in Fig. 4
11. H&E-stained control mouse (0 day) lung tissue
12. ^{1}H NMR, ^{13}C NMR and LC-MS characterization of the probe **CyO-Disu**
13. Comparison of the performance of the probe **CyO-Disu** and other reported work towards GSH.
14. References

1. General methods

Materials: The solution of the probe **CyO-Disu** (1 mM) could be dissolved in dimethyl sulfoxide (DMSO) and maintained in the refrigerator at 4 °C. The purity of the probe was tested on a Shimadzu LC-20AT HPLC system equipped with fluorescence and UV-vis absorption detectors. When it was used for imaging, the purity of our probe was greater than 99.89%. Superoxide ($O_2^{\cdot-}$) was created by the enzymatic reaction of xanthine/xanthineoxidase (XA/XO; 6.0 μM/3 mU) at 25 °C for 5 min.[1,2] ·OH was generated by Fenton reaction between Fe^{II}(EDTA) and H_2O_2 quantitively, and Fe^{II}(EDTA) concentrations represented ·OH concentrations. *Tert*-butylhydroperoxide (*t*-BuOOH) and cumene hydroperoxide (CuOOH) could also be used to induce ROS in biological systems. The $ONOO^-$ source was the donor 3-Morpholinosydnonimine hydrochloride (SIN-1, 200 μmol/mL).[3] NO was generated in form of 3-(Aminopropyl)-1-hydroxy-3-isopropyl-2-oxo-1-triazene (NOC-5, 100 μM/mL).[4] NO_2^- was generated from $NaNO_2$. OCl^- was standardized at pH 12 ($\varepsilon_{292\ nm}$ = 350 $M^{-1}cm^{-1}$).[5] Methyl linoleate (MeLH) and 2,2'-azobis-(2,4-dimethyl)valeronitrile (AMVN) were used to produce MeLOOH.[6,7] H_2O_2 was determined at 240 nm ($\varepsilon_{240\ nm}$ = 43.6 $M^{-1}cm^{-1}$). $^1O_2$ was generated from 3,3'-(naphthalene-1,4-diyl)dipropionic acid.[8] Angeli's salt (an HNO donor) was prepared as reported by King and Nagasawa and stored dry at - 20°C in a refrigerator.[9] All the reagents were obtained from Aladdin (USA). All other chemicals were from commercial sources and of analytical reagent grade unless indicated otherwise. The stock solutions were diluted to desired concentrations when needed. HEPES (4-(2-Hydroxyethyl)-1-piperazineethanesulfonic acid) was obtained from Aladdin. 3-(4,5-Dimethylthiazol-2-yl)-2,5-diphenyltetrazolium bromide (MTT) was purchased from Sigma-Aldrich. DMEM (Dulbecco's Modified Eagle Medium, #SH30022.01) was brought from HyClone. Fetal Bovine Serum (FBS, #10439024) was brought from Thermo Fisher Scientific. VEGF Receptor 2 (D5B1) Rabbit mAb (PE Conjugate) was obtained from Cell Signaling Technology (#12634). Ultrapure water was used throughout.

Instruments: Absorption spectra were obtained on Lambda 35 UV-visible spectrophotometer (PerkinElmer). Fluorescence spectra were measured by FluoroMax-4 Spectrofluorometer with a Xenon lamp and 1.0-cm quartz cells. ^1H and ^{13}C NMR spectra were taken on a Bruker spectrometer. High-resolution mass spectra were carried on the LCQ Fleet LC-MS System (Thermo Fisher Scientific). The fluorescence images of cells were acquired using an LTE confocal laser scanning microscope (Olympus FV1000 confocal laser-scanning microscope) with an objective lens (× 40/60). Flow cytometry data were collected by BD Biosciences FACSAria. Ultrathin sections were cut using Leica EM UC7. BALB/c mice and nude mice fluorescence and x-ray images were collected by Bruker In-vivo Imaging System. Mice pathological sections were imaged by Nikon Model Eclipse Ci-L Microscope.

Spectral experiments.

All the photophysical characterization experiments were carried out at 37°C. Ultrapure water was used to prepare all aqueous solutions. 4-(2-hydroxyethyl)-1-piperazineethanesulfonic acid (HEPES, 10 mM) was purged with N_2 for 5 min before use. Absorption spectra were obtained with 1.0-cm glass cells. Fluorescence emission spectra were obtained with a Xenon lamp and 1.0-cm quartz cells. The fluorescence intensity were measured at $\lambda_{ex/em}$ = 710/750-825 nm and at $\lambda_{ex/em}$ = 535/560-700 nm, respectively. **CyO-Disu** (0.10 mL, 1.0 mM) was added to a 10.0-mL color comparison tube. After dilution to 10 μM with 10 mM HEPES buffers, analytes were added. The mixtures were equilibrated six mins before measurement.

Cell culture: HL-7702 cells (human normal liver cell line), human hepatocellular liver carcinoma cell line (SMMC-7721), rat liver cell line (BRL 3A) and rat hepatoma cell line (RH-35) were purchased from the Committee on Type Culture Collection of Chinese Academy of Sciences (Shanghai, China). RH-35 cells were incubated in DMEM supplemented with 10% fetal bovine serum (FBS). The cultures were maintained at 37 °C in a 95% humidified

atmosphere with 5% CO_2.

Isolation and culture of hepatocytes: The primary hepatocytes were acquired from 6- to 8-weeks-old female BALB/c mice. Hepatocytes were isolated by the *in situ* collagenase perfusion method.[10] Primarily, the liver was perfused by perfusion buffer and collagenase buffer through a needle aligned along the inferior vena cava. Then the liver was dissected, suspended in Hanks solution and filtered through cheesecloth and 100 mm nylon membrane to remove connective tissue debris and cell clumps. Hepatocytes were purified by centrifugation (42 *g* force, 2 min) for three times at 4 °C and then by a density gradient centrifugation (42 *g* force, 2 min) at 4 °C using 45% Percoll solution. The isolated hepatocytes (25,000 cells/cm^2) were allowed to adhere onto 20 mm Petri-dishes in Williams' Medium E, pH 7.3, containing 10 mM $NaHCO_3$, 50 mg/ml penicillin and streptomycin, and 100 mg/mL neomycin (WE medium) under humidified atmosphere of 5% CO_2 and 95% air for 3 h at 37 °C. Fresh WE medium was added to remove non-adherent hepatocytes. And the adherent cells were cultured for an indicated time.[11]

Flow cytometry analysis: The cells were cultured at 2.0×10^5 cells/well in 6-well plates, and then treated with probes as described in the paper. After harvest, cells were washed and suspended in fresh complete medium and analyzed by flow cytometry. For channel 1: the excitation wavelength was selected 633 nm and the collected wavelengths were selected 750 - 810 nm. For channel 2: the excitation wavelength was selected 633 nm and the collected wavelengths were selected 650 - 670 nm.

Histological experiments: Liver and lung tissues from mice were excised. The tissues were fixed in 10% formaldehyde and embedded in paraffin. Then the paraffin masses were cut and dewaxed. The sections were dehydrated using graded ethanol series and washed by distilled water. The tissue sections were stained with hematoxylin and eosin to observe the normal and tumor tissue structure. Immunofluorescence staining followed the dehydration. After being treated with Triton X-100 and serum, the sections were stained by Ki-67 (D3B5) Rabbit mAb (Alexa Fluor® 647 Conjugate) (Cell Signaling Technology, USA) overnight. The sections were stained by DAPI to display the nucleus and enveloped by glycerol before observation.

Cell imaging. Cell fluorescent images in Fig. 2 and Fig. 3 were obtained from the Olympus FV3000 confocal laser-scanning microscope with an objective lens (40×). Cells were plated on Petri-dishes (Φ = 20 mm) and allowed to adhere for 24 h before imaging. The probe was added to the culture plates which were filled with 1 mL fresh complete medium. The ratio of fluorescence images was collected from two channels. For channel 1 (Ch 1), the excitation wavelength was 730 nm, and the emission intensities collection from 780 nm to 810 nm. For channel 2 (Ch 2), 635 nm was chosen as the excitation wavelength, and the emission wavelength range from 680 nm to 750 nm was collected. Pseudocolour ratio images were reconstructed to manifest the ratio emission intensity of channel 2 images to channel 1 image at the same time point.

Establishment of mice models of orthotopic hepatoma mouse and pulmonary metastatic hepatoma. All surgical protocols were carried out in conformity with National Guidelines for the Care and Use of Laboratory Animals. The experimental procedures were approved by the Institutional Animal Care and Use Committee, Hainan Medical University. Approval Number: HYLL-2022-385. Five-week-old female BALB/c nude mice were commercially obtained from Hainan Medical University and group-housed on a 12 h light-dark cycle and 40% - 60% relative humidity at 22°C, with free access to food and water. The murine hepatoma cell line H22 was suspended in the mixture of DMEM/Matrigel (30 μL, 1/1) and inoculated under the capsule of the left hepatic lobe. On days 0, 7, 14, 21 and 28, the mice were sacrificed and then the liver tissues were freshly frozen in liquid nitrogen, following the

staining with hematoxylin and eosin to verify orthotopic hepatoma mouse model. To evaluate the successful establishment of the pulmonary metastatic hepatoma mouse model, liver, and lung tissue sections from the mice on days 35, 42 and 49 were stained with hematoxylin and eosin.

2. The synthesis of the probe CyO-Disu.

We have outlined the probe synthesis steps, detailed synthesis procedure refers to our previous reported study: Han, X., Song, X., Yu, F., Chen, L., Chem. Sci., 2017, ***8***, 6991-7002; Han, X., Song, X., Yu, F., Chen, L., Adv. Funct. Mater, 2017, ***27***, 1700769.

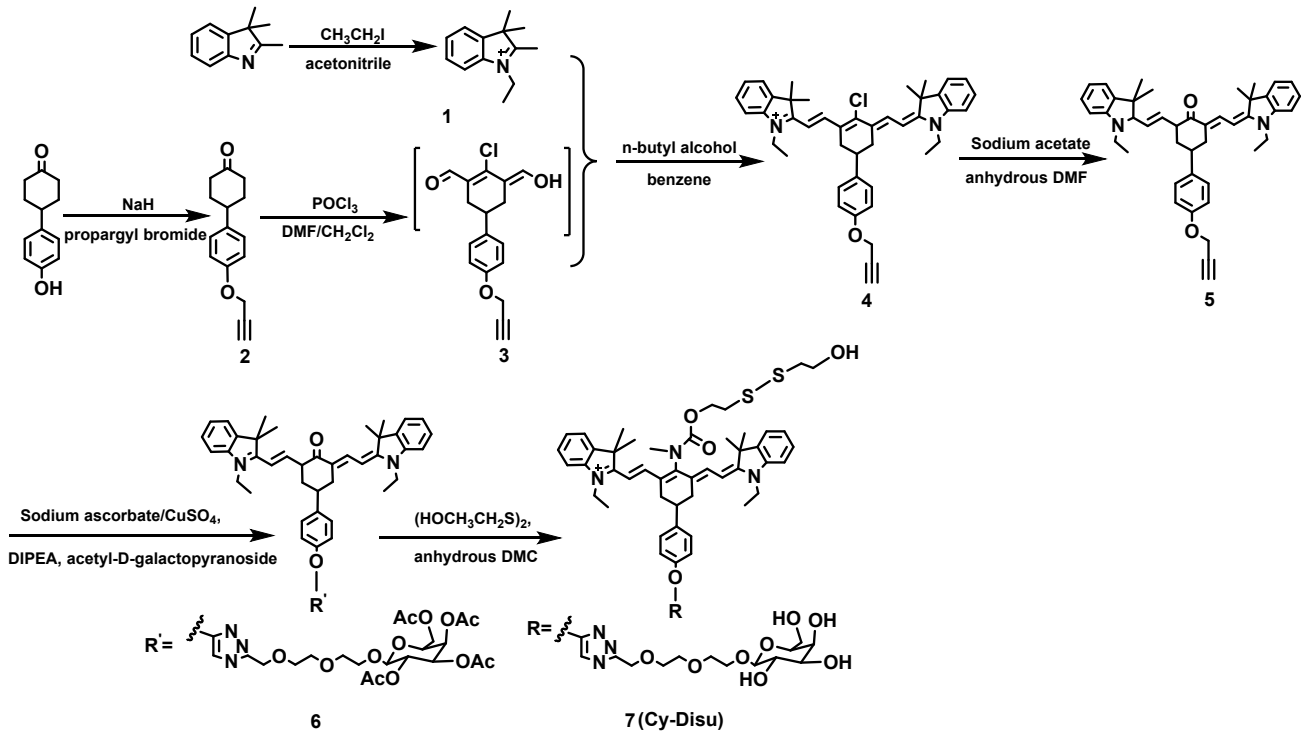

Scheme S1 The synthesis of the probe **CyO-Disu**.

3. Effect of pH values to CyO-Disu and CyO

Standard fluorescence pH titrations were performed in 10 mM HEPES solution at a concentration of 10 μM (**CyO-Disu** and **CyO**). As shown in Fig. S1, the pH of the mediums hardly effected on fluorescence intensity within the range from 3.0 to 10.0. Therefore, **CyO-Disu** would work well under physiological conditions (pH = 7.4).

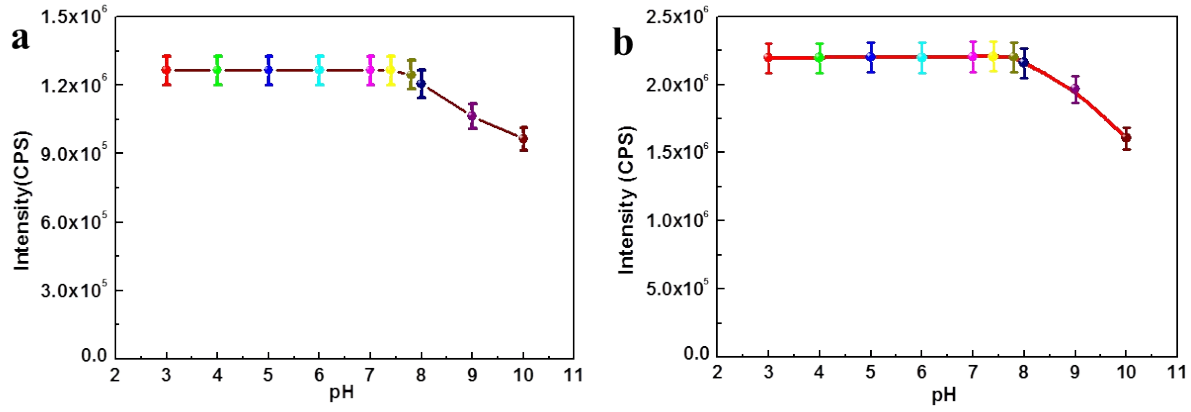

Fig. S1. Effect of pH values. a) The fluorescence emission changes at 783 nm with the pH titration curve of **CyO-Disu** (10 μM). b) The

fluorescence emission changes at 613 nm with the pH titration curve of **CyO** (10 μM). pH: 3.0, 4.0, 5.0, 6.0, 7.0, 7.4, 7.8, 8.0, 9.0, 10.0 (10 mM HEPES buffer).

4. Selectivity of CyO-Disu toward various reactive substances

The fluorescence emission and UV absorbance spectra of probe with various analytes were carried out to further verify the selectivity of the probe. The probe (10 μM) was treated with various analytes in HEPES buffer (10 mM, pH 7.4) at 37 °C. The fluorescence emission and UV absorbance spectra were recorded after 60 min. As shown in Fig. S2, reactive oxygen species, reactive nitrogen species, anions and metal ions could not induce interference.

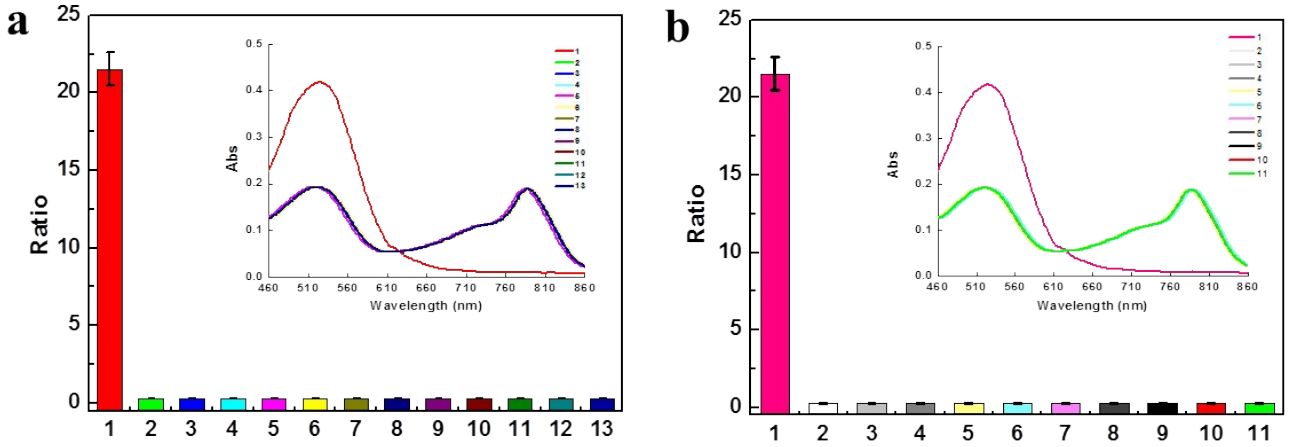

Fig. S2. Fluorescent ratio ($F_{613\ nm}/F_{783\ nm}$) response and absorbance spectra of **CyO-Disu** (10 μM) to reactive oxygen species, reactive nitrogen species, anions and metal ions in HEPES buffer (pH 7.4, 10 mM) at 37 °C. a) 1, 10 mM GSH; 2, 200 μM NO_2^-; 3, 200 μM $ONOO^-$; 4, 200 μM NO; 5, 200 μM t-BuOOH; 6, 200 μM H_2O_2; 7, 200 μM $O_2^{\cdot-}$; 8, 200 μM MeLOOH; 9, 200 μM ClO^-; 10, 200 μM CuOOH; 11, 20 μM HNO; 12, 20 μM •OH; 13, 20 μM $^1O_2$. b) 1, 20 μM GSH; 2, 1 mM K^+; 3, 1 mM Na^+; 4, 1 mM Ca^{2+}; 5, 1 mM Mg^{2+}; 6, 1 mM Zn^{2+}; 7, 1 mM Cu^{2+}; 8, 1 mM Cl^-; 9, 1 mM Br^-; 10, 1 mM F^-; 11, 1 mM CO_3^{2-}. **CyO-Disu**: $F_{783\ nm}$: λ_{ex} = 730 nm, λ_{em} = 783 nm; $F_{613\ nm}$: λ_{ex} = 535 nm, λ_{em} = 613 nm. The fluorescence emission and UV absorbance spectra were recorded after 60 min.

5. Reaction kinetics of CyO-Disu towards GSH

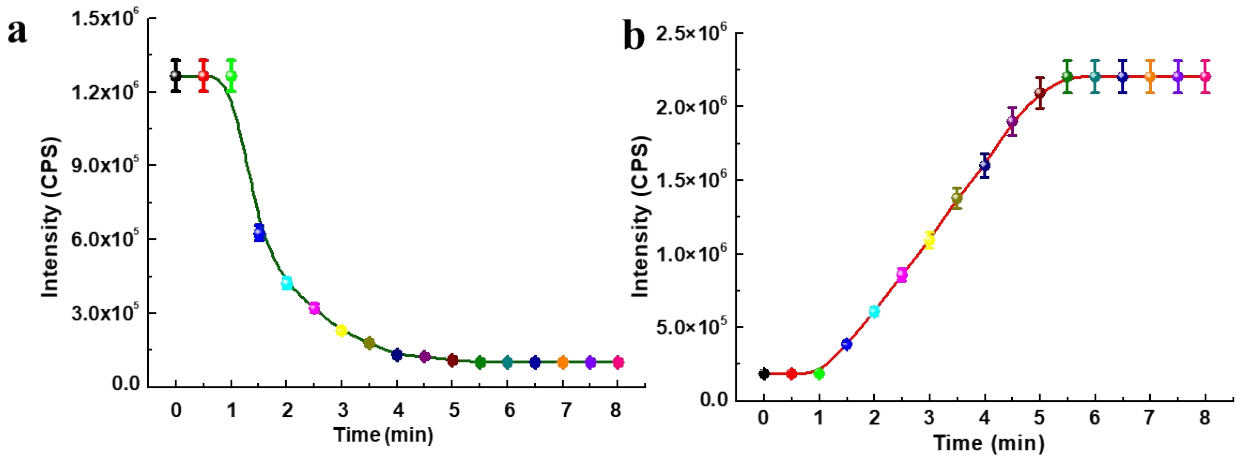

Fig. S3. Time-dependent fluorescent intensity of probe **CyO-Disu** towards GSH (10 mM) during 0 – 8 min. GSH was added at the reaction initiation in 10 mM HEPES buffer (pH 7.4). The reactions were measured during 0 - 80 s at 37 °C. **CyO-Disu**: $F_{785\ nm}$: λ_{ex} = 730 nm, λ_{em} = 783 nm; $F_{600\ nm}$: λ_{ex} = 535 nm, λ_{em} = 613 nm.

6. MTT assay for CyO-Disu

To access the potential toxicity of **CyO-Disu**, MTT assays were carried out. SMMC-7721, HL-7702, RH-35, and BRL 3A cells (10^6 cells/mL) were plated into 96-well microtiter plates in DMEM with 10% fetal bovine serum (FBS). Plates were maintained at 37 °C in a 5% CO_2/95% air incubator for 24 h. Then the cells were incubated for 24 h at 37 °C in a 5% CO_2/95% air upon different concentrations probe of 0 μM to 100 μM respectively. MTT solution (5.0 mg/mL, PBS) was then added to each well. After 4 h, the remaining MTT solution was removed, and 200 μL of DMSO was added to each well, shaking 10 min to dissolve the formazan crystals at room temperature. Absorbance was measured at 490 nm in a TECAN infinite M200pro microplate reader.

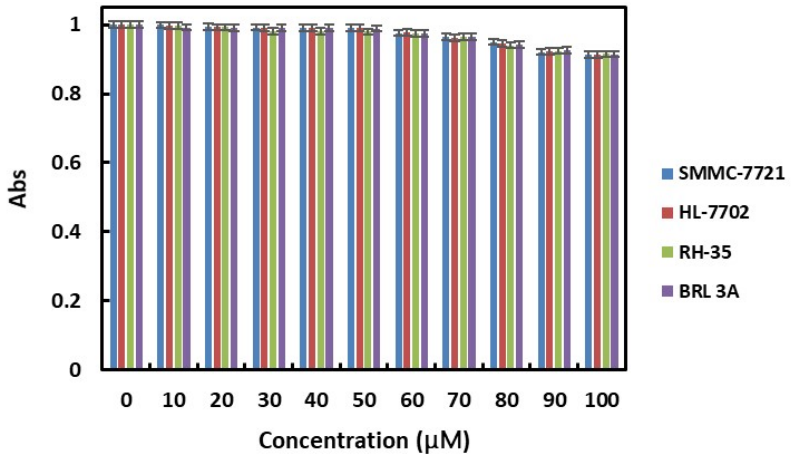

Fig. S4. MTT assay of SMMC-7721, HL-7702, RH-35 and BRL 3A cells with different concentrations of **CyO-Disu**. The data were shown as mean (± s.d.) (n = 7).

7. Quantitative assay of GSH concentration of various cells in Fig. 2a

The correlated GSH concentration of the results displayed in Fig. 2b was calculated, according to the equation lg(Ratio) = 0.173 [GSH] mM - 0.45. As illustrated in Fig. S4, the concentration of GSH was ranked as RH-35 > SMMC-7721 > BRL 3A > HL-7702. The corresponding GSH concentration of SMMC-7721 after 5 min's reaction was 7.2 mM and the fluorescent intensity ratio was 6.25 (Fig. 2b). Therefore, we can make a presumption that if the fluorescent intensity ratio was above 6.25, which represents a GSH concentration of 7.2 mM, the cells could be suggested to be hepatocellular carcinoma cells.

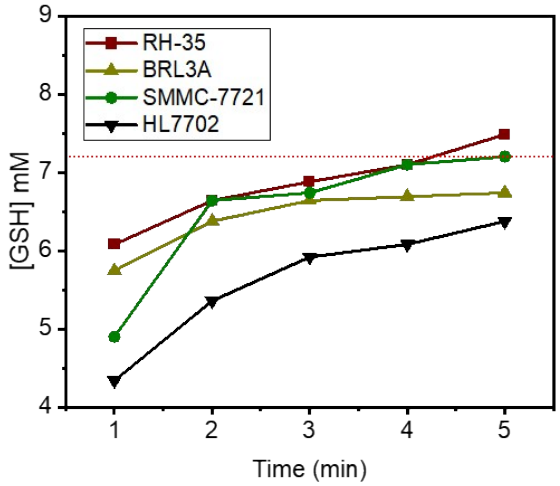

Fig. S5. Quantitative assay of GSH concentration of various cells in Figure 2a

8. Sublocation in Cells

To establish the applicability of **CyO-Disu** in subcellular studies, we performed the co-localization experiments using **CyO-Disu** (10 μM), Calcein-AM, (1 μg/mL) (a commercial cytoplasm marker) and a DNA marker Hoechst 33342 (1 μg/mL) (a commercial nuclear dye) to determine the co-localization of fluorescence emission. The cells were incubated with Hoechst 33342 for 30 min, 1 μM Calcein-AM for 10 min and **CyO-Disu** for 5 min subsequently. With the help of Image-Pro Plus software, the respective spectra acquired from the three dyes were shown in Fig. S6. The fluorescent images of **CyO-Disu** (red channel) and Calcein-AM (green channel) merged primely. Hoechst 33342 exhibited a perfect sublocation in the nucleus. The results confirmed that our probe could specifically localize in the cytoplasm. And our probe also indicated a potentially powerful approach for real-time imaging cytoplasm thiols changes in cells and *in vivo*.

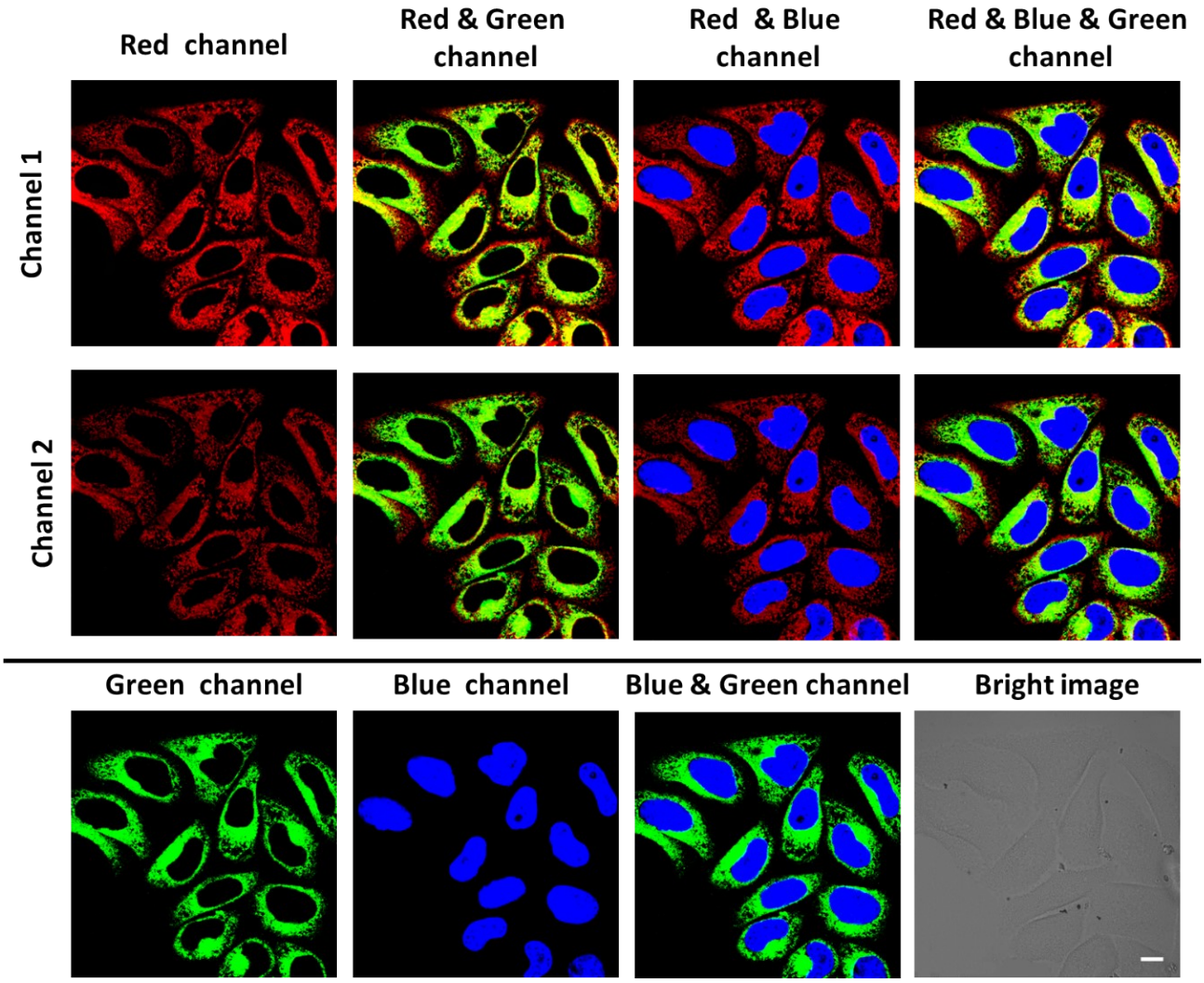

Fig. S6. Confocal microscopy images of live RH-35 costained by **CyO-Disu** (10 μM), Calcein-AM, (1 μg/mL) and Hoechst 33342 (1 μg/mL). The cells were incubated with Hoechst 33342 for 30 min, 1 μM Calcein-AM for 10 min and then **CyO-Disu** for 2 min at 37 °C subsequently and imaged with **CyO-Disu** (channel 1: λ_{ex} = 730 nm, λ_{em} = 750 - 800 nm and channel 2: λ_{ex} = 635 nm, λ_{em} = 690 - 740 nm), Calcein-AM (green channel: λ_{ex} = 488 nm, λ_{em} = 500 - 550 nm) and Hoechst 33342 (blue channel: λ_{ex} = 405 nm, λ_{em} = 425 - 525 nm). Fluorescent images of RH-35 were acquired on the Olympus FV1000 confocal laser-scanning microscope with an objective lens (× 60). Scale bar: 10 μm.

9. Bright-field Images of Fig. 2 and Fig. 3

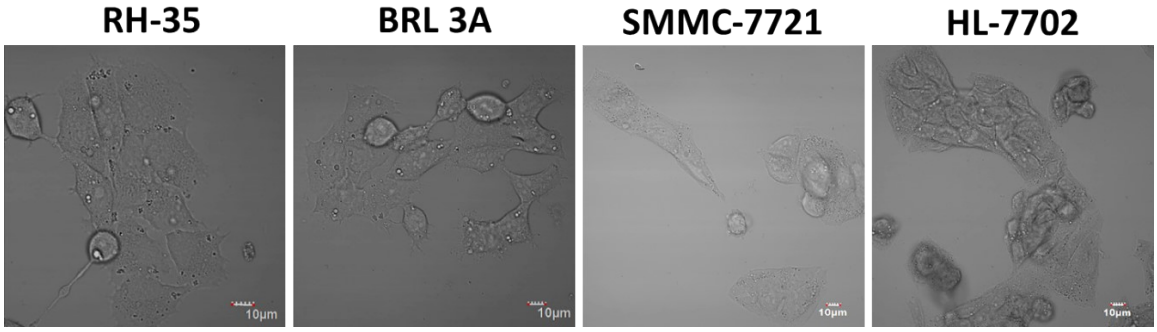

Fig. S7. Bright-field images of Fig. 2. Scale bar: 10 μm.

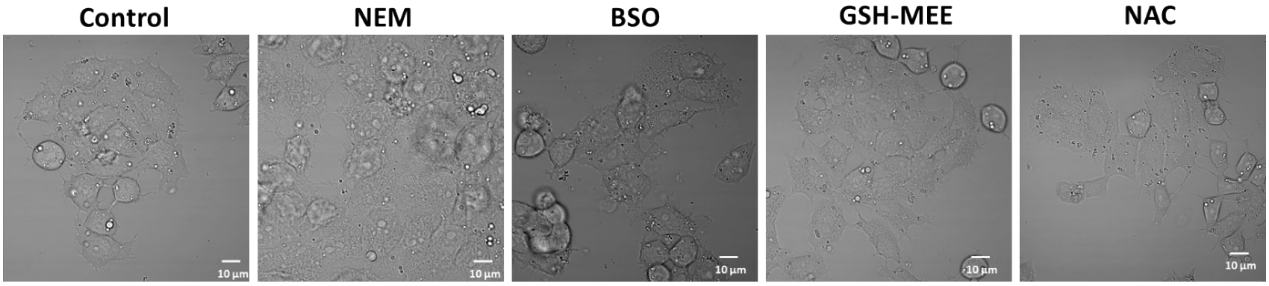

Fig. S8. Bright-field images of Fig. 3. Scale bar: 10 μm.

10. H&E -stained liver tissues in Fig. 4

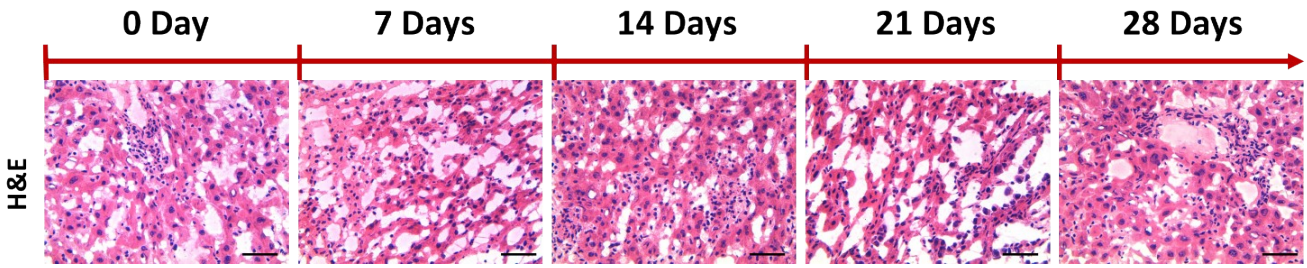

Fig. S9. Representative slides of H&E-stained liver tissues in Fig. 4. Scale bar: 50 μm.

11. H&E-stained control mouse (0 day) lung tissue

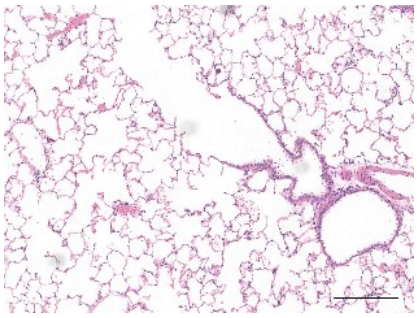

Fig. S10. Representative slides of H&E-stained control mouse (0 day) lung tissue. Scale bar: 200 μm.

12. ^{1}H NMR, ^{13}C NMR and LC-MS characterization of the probe CyO-Disu

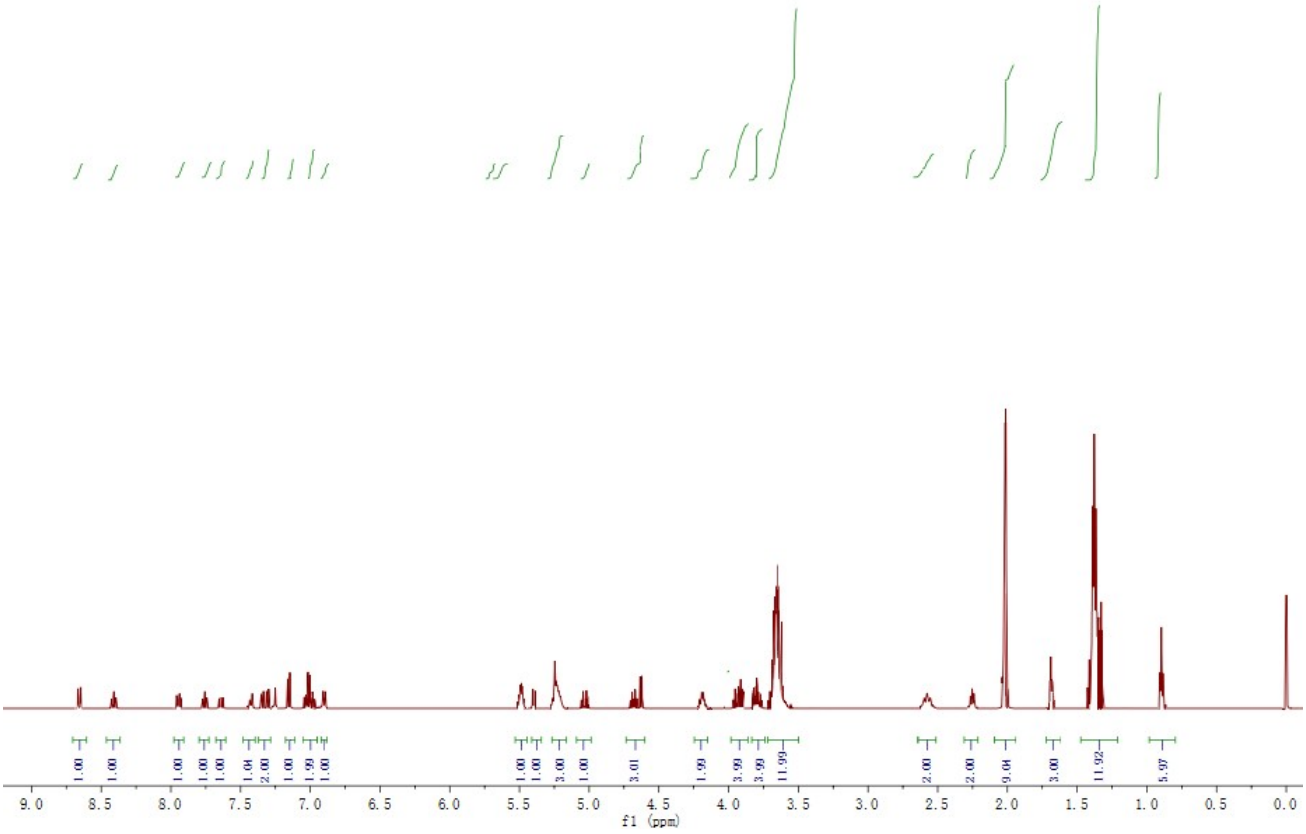

Fig. S11 ^{1}H NMR characterization of the probe **CyO-Disu.**

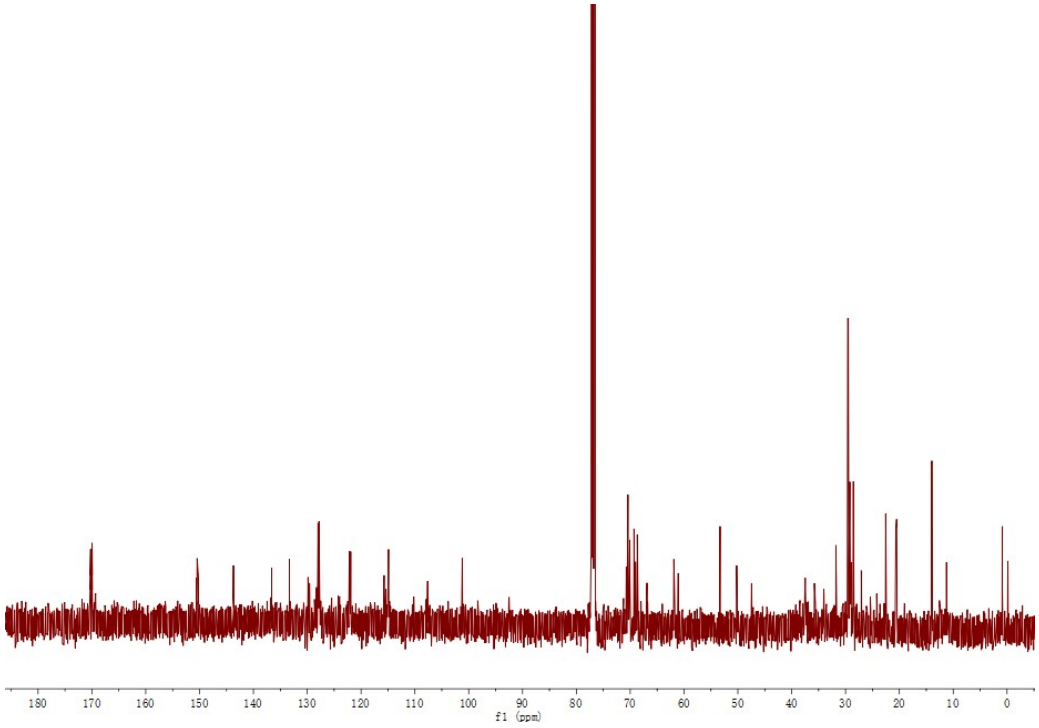

Fig. S12 ^{13}C NMR characterization of the probe **CyO-Disu.**

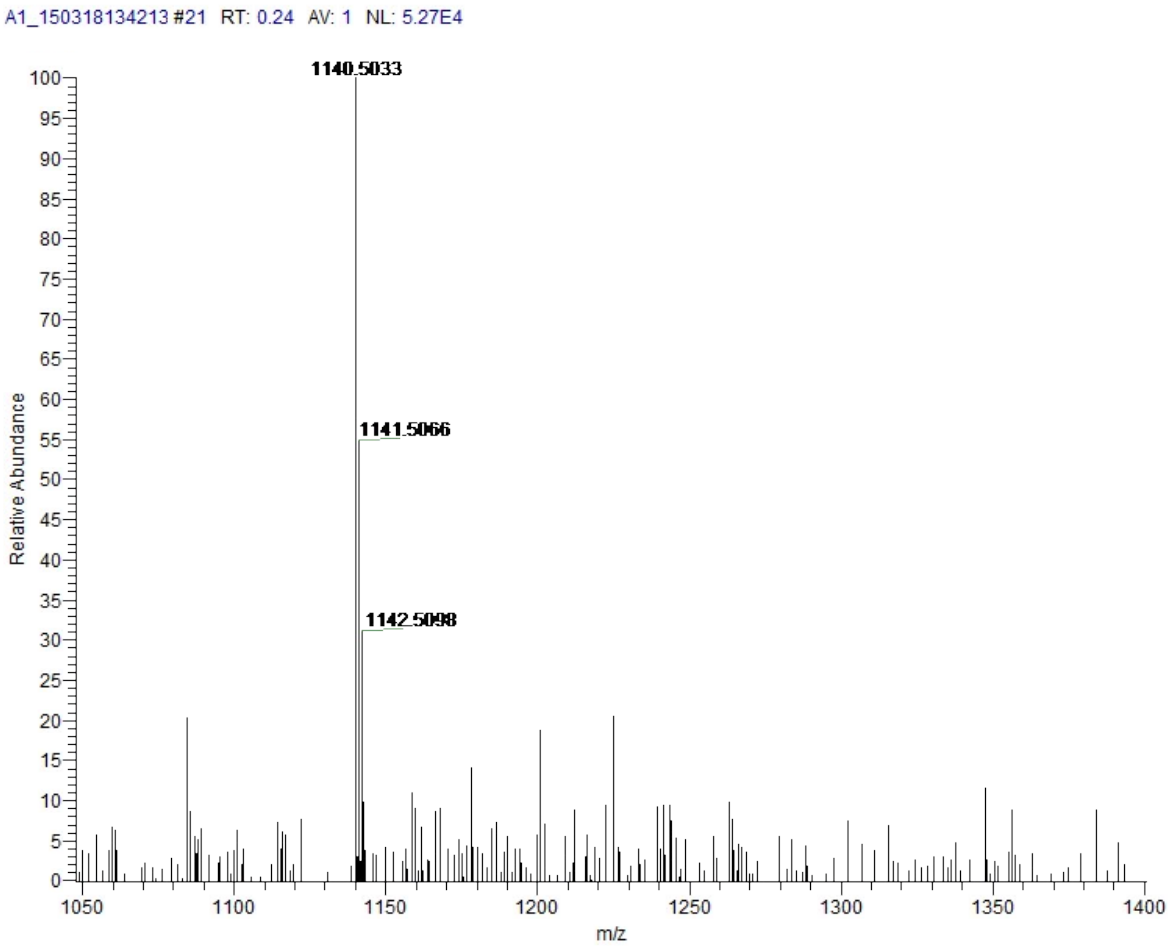

Fig. S13 LC-MS characterization of the probe **CyO-Disu.**

13. Comparison of the performance of the probe CyO-Disu and other reported work towards GSH.

Probe	$\lambda_{ex}/\lambda_{em}$ (nm)	Sensitivity	Reaction kinetics	Bioapplication	Ref.
NTR-AHC	365/463	5 μM	> 20 min	NA	12
Coumarin derivative 1	400/613	5 mM	30 min	Living cells & rat hippocampal slice	13
Cou-Br	462/520	79 μM	5 min	Living cells, mice model and clinical tissue specimen	14
NIR-HMPC	645/731	0.39 μM	5 min	Living cells and mice model	15
CyO-Dise	530/615	10 mM	30 min	Living cells and mice model	16
CyO-Disu	535/613	65 nM	5 min	Living cells and mice model	This work

14. References

1. Massey, V.; Edmondson, D. J. *Biol. Chem.* **1970**, *245*, 6595-6598.
2. Edmondson, D.; Massey, V.; Palmer, G.; Beachan III, L. M.; ELion, G. B. *J. Biol. Chem.* **1972**, *247*, 1597-1604.
3. Uppu, R. M. *Anal. Biochem.* **2006**, *354*, 165-168.
4. Maeda, H.; Yamamoto, K.; Nomura, Y.; Kohno, I.; Hafsi, L.; Ueda, N.; Yoshida, S.; Fukuda, M.; Fukuyasu, Y.; Yamauchi Y.; Itoh, N. *J. Am. Chem. Soc.* **2005**, *127*, 68-69.
5. Morris, J. C. *J. Phys. Chem.* **1966**, *70*, 3798.
6. Terao, J. A.; Nagao, A.; Park D. K.; Lim, B. P. *Meth. Enzymol.* **1992**, *213*, 454- 460.
7. Chance, B.; Sies, H.; Boveris, A. *Proc. Natl. Acad. Sci. U.S.A.* **1988**, *85*, 3175-3179.
8. J. M.; Cazin, B.; Duprat, F. *J. Org. Chem.* **1989**, *54*, 726-728.
9. King, S. B.; Nagasawa, H. T. *Methods. Enzymol.* **1999**, *301*, 211-220.
10. Seglen, P. O. *Methods Cell Biol.*, **1976**, *13*, 29-83.
11. Hoshiba, T.; Cho, C. S.; Murakawa, A.; Okahata Y.; Akaike, T. *Biomaterials*, **2006**, *27*, 4519-4528.
12. Tian, X., Kumawat, L. K., Bull, S. D., Elmes, R. B. P., Wu, L., James, T. D., *Tetrahedron*, **2021**, 82, 131890.
13. Kwon, N., Lim, C. S., Lee, D., Ko, G., Ha, J., Cho, M., Swamy, K. M. K., Lee, E.-Y., Lee, D. J., Nam, S.-J., Zhou, X., Kim, H. M., Yoon, J., *Chem. Commun.*, **2022**, 58, 3633-3636.
14. Zou, Y., Li, M., Xing, Y., Duan, T., Zhou, X., Yu, F., *ACS Sens.*, 2020, 5, 242-249.
15. Yang, Y., Zhou, T., Jin, M., Zhou, K., Liu, D., Li, X., Huo, F., Li, W., Yin, C., *J. Am. Chem. Soc.*, **2020**, 142, 1614-1620.
16. Han, X.; Song, X.; Yu, F.; Chen, L. *Chem. Sci.*, **2017**, 8, 6991-7002.